

# Survey of Data on Primary Cosmic-Ray Nuclei above $10^{14}$ eV

A. M. Hillas

*Phil. Trans. R. Soc. Lond. A* 1975 **277**, 413-428

doi: 10.1098/rsta.1975.0007

## Email alerting service

Receive free email alerts when new articles cite this article - sign up in the box at the top right-hand corner of the article or click [here](#)

Survey of data on primary cosmic-ray nuclei above  $10^{14}$  eV

BY A. M. HILLAS

*Department of Physics, University of Leeds*

Primary cosmic-ray particles, detected by means of the extensive cascades they generate in the atmosphere, have been observed over a continuous range of energies up to  $10^{20}$  eV, and apparently somewhat higher. At energies such that the radius of curvature of their trajectories, if they are protons, as expected, is comparable to our distance from the galactic centre, the arrival directions of 84 observed particles are distributed randomly over the sky.

The energy spectrum of the particles shows an anomaly near  $10^{15}$  eV, where the flux is higher than expected by extrapolation of data near  $10^{12}$  eV, and then falls very rapidly (spectral exponent  $\gamma \approx 3.5$  at energies just above  $4 \times 10^{15}$  eV). Above  $10^{17}$  eV the flux falls off less rapidly,  $\gamma$  being near 3.0 in the range  $10^{18}$  to  $3 \times 10^{19}$  eV. Extrapolating the flux back to low energies from  $10^{18}$  eV, where the particles are often assumed to be of extra-galactic origin, gives a flux higher than that actually observed at low energies. The best evidence on energies of the large showers indicates that these are above  $10^{20}$  eV, which is greater than the upper limit to which metagalactic protons could survive interactions with microwave photons. There is evidence that many of the most energetic particles (near  $10^{18}$  eV) are indeed protons, but this result is only preliminary.

## 1. BACKGROUND

Cosmic-ray particles have been detected over a continuous range of energy up to  $10^{20}$  eV, although above  $10^{14}$  eV the particles are observed indirectly, by means of the extensive showers of secondary particles which they generate on entering the atmosphere. Direct observation of the primary particles in space appears impracticable above  $10^{16}$  eV, for the flux of particles above this energy is about  $1 \text{ m}^{-2} \text{ sr}^{-1}$  per year, and the direct observations have not yet reached  $10^{16}$  eV. However, the shower of particles resulting from atomic collisions in the atmosphere can sometimes be detected at distances up to 2 km from the trajectory of the primary particle, when it reaches the ground, making possible collecting areas of tens of square kilometres using a few widely spaced particle detectors, although particles whose energy exceeds  $10^{20}$  eV may arrive at a rate not much above 1 per  $100 \text{ km}^2$  per year. Shower observations give a particle's energy to tolerable accuracy, and its direction of arrival to within a few degrees, but the nature of the primary particle is proving much more difficult to decide.

The framework within which observations were discussed a few years ago may be summarized as follows. At the London conference, Greisen (1965) presented the energy spectrum of primary cosmic rays as having three sections, in each of which the particle flux in the energy range  $E$  to  $E+dE$  varied as  $E^{-\gamma}dE$ , with  $\gamma = 2.6$  for  $E < 3 \times 10^{15}$  eV, changing to 3.2 until an energy near  $10^{18}$  eV; then the spectrum levelled off somewhat to  $\gamma = 2.6$  again at the highest energies. The point of steepening of the spectrum, near  $3 \times 10^{15}$  eV, is often referred to as the 'knee' of the spectrum: it was first established by Kulikov & Khristiansen (1958) and the most widely held explanation was that most particles were accelerated in the Galaxy, and trapped within it for long periods by magnetic fields, but that particles of magnetic rigidity exceeding  $3 \times 10^{15}$  eV, escaped more rapidly. One would then expect iron nuclei present in the primary

radiation to be efficiently trapped up to about  $10^{17}$  eV (for the same magnetic rigidity), and between  $3 \times 10^{15}$  eV and  $10^{17}$  eV the primary radiation might thus become progressively depleted of light nuclei. There had then been only one experiment to determine the energy spectrum much above  $10^{17}$  eV, at Volcano Ranch, and Linsley (1963) had reported a distinct flattening operative for energies above  $10^{18}$  eV, which was widely interpreted as a flux of particles originating outside our Galaxy, with a spectrum paralleling the galactic flux at lower energies, but 30 times lower in intensity. Such energetic particles were expected to be protons, as nuclei were subject to photodisintegration on starlight. But even protons should suffer severe energy losses which should depress their spectrum sharply near  $10^{20}$  eV if they are not trapped locally, because of interactions with the universal microwave radiation (Greisen 1966; Zatsepin & Kuzmin 1966).

To test this general picture, various experiments have sought to detect changes in the nature of the particles around  $10^{16}$  eV, and near  $10^{18}$  eV, to find whether the flux declined sharply near  $10^{20}$  eV, and to measure anisotropies in the arrival directions at the highest energies, where magnetic deflexions should become less effective; and in general, the greatest interest attaches to those aspects of shower experiments which may determine whether cosmic rays, or some component of them, are of extragalactic origin, or which may point to some other special source.

Recent work at lower energies has revealed a spectrum falling rather more rapidly than previously thought, making the flux near  $10^{15}$  eV appear to stand out more like a peak, which Karakula, Wdowczyk & Osborne (1973) have interpreted as possibly a component originating in pulsars.

## 2. ISOTROPY OF THE PRIMARY RADIATION AT VERY HIGH ENERGIES

In a magnetic field of  $3 \times 10^{-10}$  T, typical of the galactic disk, a  $3 \times 10^{19}$  eV proton travelling normally to the field would move in an arc of radius 9 kpc, which is comparable to our distance from the galactic centre, and about 20 times the thickness of the radio disk. Outside the disk the magnetic field strength is presumed to be weaker, from the weakness of synchrotron radiation, so the particles would suffer less deflexion, and in this energy range the arrival directions of protons should reflect the distribution of their sources, if they lie within the Galaxy.

Many particles of this energy have now been recorded by the largest air shower experiments. The direction of arrival of a primary particle is typically measured to about  $4^\circ$  accuracy in the experiments to be quoted, and is found from the time intervals between the arrival of the shower at several detectors, as the shower particles propagate in a saucer-shaped disk moving forward at the speed of light. Bell *et al.* (1973*a*) have given the arrival directions of the fifty most energetic showers detected within  $60^\circ$  of the zenith by the Sydney group, and, in the Southern Hemisphere they are well placed to view the galactic centre. Although the precise energy to be ascribed to these showers is still under discussion, the threshold energy will be taken as  $2 \times 10^{19}$  eV: the degree of uncertainty is unimportant in this context. In figure 1 these shower directions have been plotted on a diagram of the sky in which the scale is adjusted so that each belt of declination covers an area proportional to the illumination a horizontal area would receive from those parts of that belt of declination that are within  $60^\circ$  of the zenith, if all the sky were equally bright. On such an 'equal exposure' chart, showers should appear randomly distributed over its area if cosmic rays are isotropic, assuming the showers of this

energy to be detected with equal efficiency for all zenith angles, over a fixed collecting area. (Actually this is not quite the case.)

One gains a first impression that there may be a distinct group of particles arriving from directions near the line joining the galactic centre to the south galactic pole. (If the particles are protons, at the median energy represented they might arrive  $30^\circ$  S of the galactic centre if they originated near the centre and travelled through an average field of  $3 \times 10^{-10}$  T directed circumferentially but opposite in sense to the local field.) However, the mean separation,  $s$ , of points on the diagram, and the mean closeness,  $(a+s)^{-1}$  (with the constant  $a$ , to remove infinities, taken as one tenth of the radius of the diagram), are just as expected for a random distribution of points, so there is no significant anisotropy, and the authors have not claimed one.

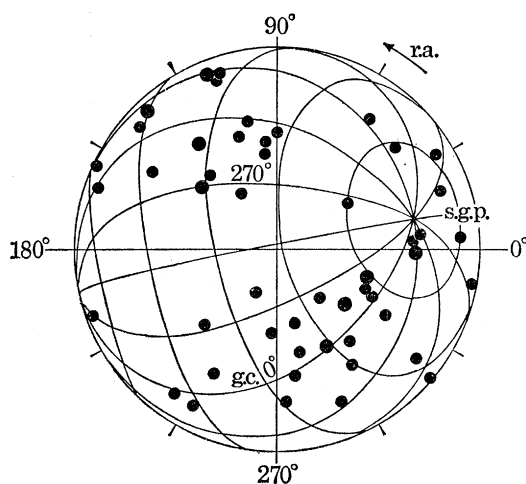


FIGURE 1. Equal exposure chart of arrival directions of showers at Sydney:  $E > 2 \times 10^{19}$  eV.

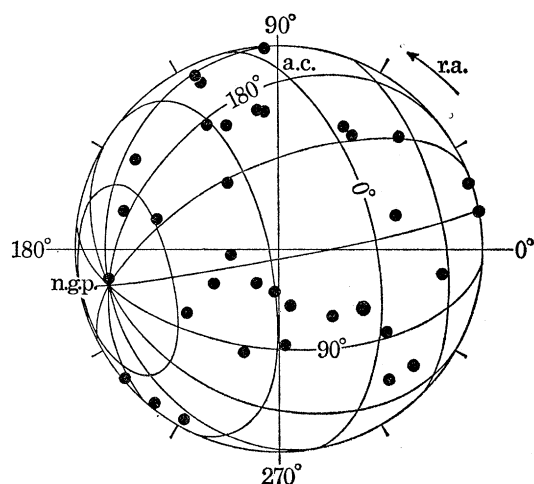


FIGURE 2. Equal exposure chart of arrival directions of showers at Haverah Park:  $E > 10^{19}$  eV.

A similar equal exposure chart for showers recorded at Haverah Park, in the northern hemisphere, is shown in figure 2. To get a reasonable number of showers the threshold has been lowered to  $10^{19}$  eV. The plot was made at the time of the Leeds Conference on Extensive Air Showers in 1970, but the sample is almost identical with that published by Lapikens *et al.* (1971). The distribution appears random.

A complete view of the sky may be presented, by combining the observations of the Sugar (Sydney), Haverah Park and Volcano Ranch detectors, adding 20 showers from Haverah Park and 14 from Volcano Ranch to the 50 from Sugar, all estimated to correspond to the same energy range. A compilation has been made by Watson & Linsley (to be published: I am indebted to them for a list of showers, which includes seven previously unpublished Volcano Ranch showers), who attempted to equalize the energy thresholds for shower selection by the three experiments by choosing thresholds which gave the same integral flux ( $4.6 \times 10^{-15} \text{ m}^{-2} \text{ s}^{-1} \text{ sr}^{-1}$ ), corresponding to about  $2 \times 10^{19}$  eV. An equal exposure chart is plotted for the combined observations in figure 3. Inevitably, any real difference in flux between the northern and southern (geocentric) hemispheres should be masked by this procedure of normalization by rates (involved also in constructing the diagram, which assigns to the sky zones observed by the various experiments areas proportional to the numbers of showers detected by the

experiments). With this reservation, one may look for anisotropies: an isotropic radiation should yield a uniform distribution of showers on the diagram.

The sky diagram may be divided into halves in various ways related to galactic coordinates, and the numbers of showers counted, with the following results. Bracketed figures refer to showers which I estimate to be above  $8 \times 10^{19}$  eV on information available (shown by larger symbols on the diagrams). In galactic latitudes less than  $30^\circ$  there are 36 (7) showers: above  $30^\circ$ , 48 (7). In the inner galactic hemisphere (within  $90^\circ$  of the galactic centre) there are 40 (6): in the outer, 44 (8). At galactic longitudes  $< 180^\circ$  ('inward arm') 44 (8):  $> 180^\circ$ , 40 (6).

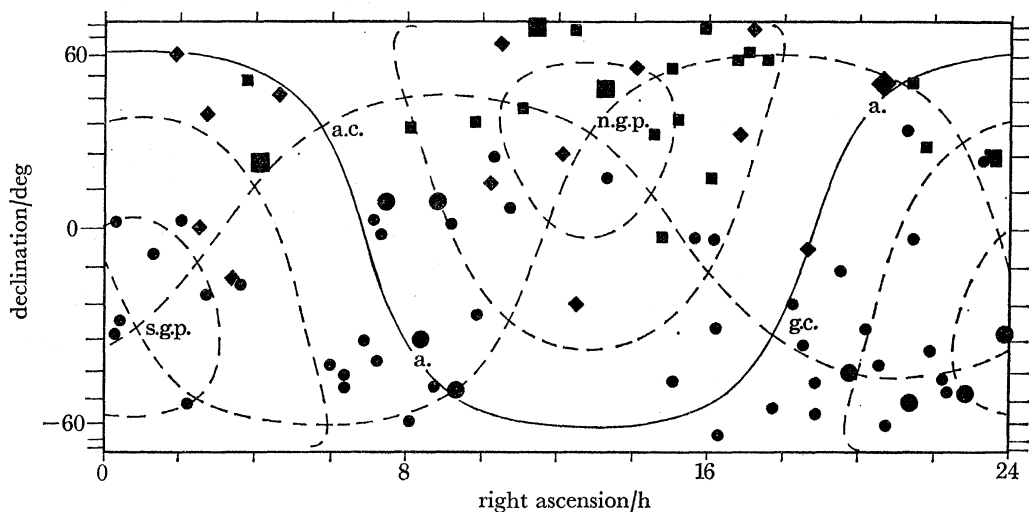


FIGURE 3. Arrival directions of showers above  $2 \times 10^{19}$  eV observed at Sydney (circles), Haverah Park (squares) and Volcano Ranch (diamonds). Larger points represent showers estimated to be above  $8 \times 10^{19}$  eV. An isotropic radiation would give points equally distributed over the area of the diagram. The galactic centre, anticentre, arm directions and poles are marked, as are lines of latitude at  $30^\circ$  intervals.

There is no evident correlation with the Galaxy in these distributions, however, the near equality of numbers of particles detected coming out from the inner hemisphere, and those moving into the Galaxy, could arise artificially from the process of energy normalization between northern and southern observations, since Haverah Park sees mostly the outer hemisphere (see figure 2). If one moves round the boundary dividing the inner and outer hemispheres by  $33^\circ$  to the lines of galactic longitude  $123^\circ$  and  $303^\circ$ , the exposure to these two regions is equal at any latitude, and the numbers are 46 (7) in the inner half ( $303^\circ$ – $360^\circ$ – $123^\circ$ ) and 38 (7) in the other, and there is still no significant difference. There is thus no indication of any outward drift from the Galaxy, or of any disk structure. Nor is there any obvious excess from the direction of the Coma cluster of galaxies, close to the north galactic pole. A direct comparison of north and south galactic hemispheres is again biased, but the Sydney chart (figure 1) has 15 out of 50 showers in the northern galactic hemisphere, where on an area basis one expects 19. The statistics are very small. Particles of near  $10^{20}$  eV have been recorded from directions close to the two galactic poles.



## 3. ENERGY SPECTRUM OF THE PRIMARY RADIATION

In this paper,  $J(E)dE$  will represent the differential intensity – the flux of particles in the energy range  $E$  to  $dE$  – while  $I(E)$  will represent the integral flux of particles of energy greater than  $E$ . As the spectrum falls so steeply it is useful to plot  $E^{1.5}I(E)$  or  $E^{2.5}J(E)$ , so that the graph is more nearly level and small but significant peculiarities are visible. Figure 4 shows a small selection of differential energy spectra which have been published, both below and above  $10^{14}$  eV, an energy which divides air shower experiments from those which make more direct contact with the primary particles. Because of the discrepancies between the published spectra, some of the methods of energy calibration will be examined and the experiments can be shown to be in much better agreement than at first appears. The arrow marked ' $E \times 2$ ' shows how any point must be displaced if the shower rate is measured correctly, but the assigned energy requires doubling. The most probable spectrum, obtained from the comparison of experiments, will be shown in figure 11.

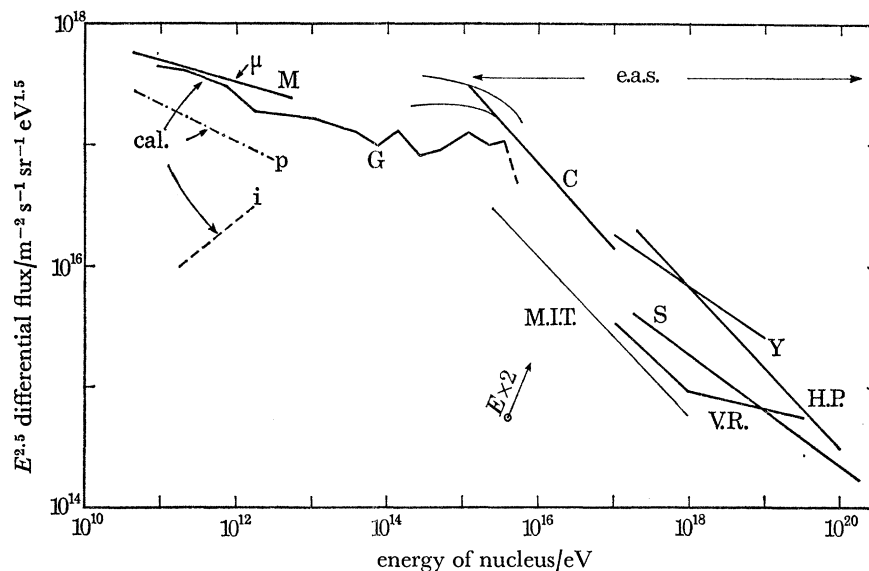


FIGURE 4. A selection of published primary energy spectra. All types of primary particle are included, except in the spectra *i* and *p*. Ionization calorimeter results: *G* (Grigorov *et al.* 1971), *p* (protons only) and *i* (iron only) from the Goddard Space Flight Center. *M* is the spectrum of all nuclei derived from sea level muons (see text). From air shower measurements: *C*, Chacaltaya (LaPointe *et al.* 1968); *M.I.T.* (Clark *et al.* 1961); *V.R.*, Volcano Ranch (Linsley 1963); *H.P.*, Haverah Park (Edge *et al.* 1973); *S*, Sydney (Bell *et al.* 1973*b*); *Y*, Yakutsk (Krasilnikov 1973). The region in which the spectra depend on extensive air shower (e.a.s.) data is indicated.

(a) Relations to spectrum below  $10^{14}$  eV

An important feature of the spectra below  $10^{14}$  eV is that the more recent measurements, using ionization calorimeters flown above or near the top of the atmosphere, have produced spectra with  $\gamma = 2.75$  (where  $J \propto E^{-\gamma}$ ), steeper than older assumed values, and apparently aiming to fall below the flux given by air shower experiments at  $10^{15}$  eV. The pioneering work of Grigorov's group with calorimeters in the proton satellites (reported recently by Grigorov *et al.* 1971) gave the spectrum *G*, extending up to  $10^{15}$  eV (though at this energy much of the cascade must leak out of the small calorimeter). (Published values of  $I(E)$  were converted to  $EJ$

by multiplying by  $(\gamma - 1)$ , except for a few points at the highest energies which were converted to  $J$  by differencing.) Up to  $2 \times 10^{12}$  eV there is confirmation from the calorimeter of the Goddard Space Flight Center (Ryan, Ormes & Balasubrahmanyam 1972), whose spectrum of proton component is shown as curve p. They have published results for several other nuclei, including the interesting case of iron (curve i: Balasubrahmanyam & Ormes 1973). If their spectrum for iron ( $\gamma = 2.0$ ) is extrapolated it may meet the air shower spectrum at  $10^{14}$  eV, and account for the high flux level seen in air shower experiments, a point which will be taken up later.

The spectrum of muons reaching the ground can be measured to beyond  $10^{12}$  eV and gives the spectrum of pions produced in the collisions of primary nuclei. Ramana Murthy & Subramanian (1972) have used recent accelerator data, extrapolated somewhat by scaling, to calculate from this the spectrum of primary nucleons (whether bound or unbound not being differentiated), and their flux has been multiplied by 1.55 to give the flux of nuclei having the same energy, this factor being appropriate to the nuclear composition near  $10^{12}$  eV. The result is plotted in line M on figure 4: its spectral exponent,  $\gamma$ , is somewhat smaller than that of the proton component, again as though heavy nuclei are becoming more important with increasing energy. One should note, however, that the Utah group disagree with this conclusion (Elbert *et al.* 1973).

(b) *Energy deposition in the atmosphere*

The most direct method of determining the energy of the particle generating a shower would be to measure the total energy deposited by its secondary particles in the atmosphere, and add the small fraction of energy remaining unabsorbed at the ground. Over 80 % of the initial energy of a large air shower should be dissipated in ionization in the atmosphere.

The growth and decay of the number,  $N$ , of charged particles in showers is illustrated in figure 5, in which the circles give results from the Chacaltaya experiment (La Pointe *et al.* 1968) for showers observed under various thicknesses of air (various angles of inclination) but supposed to have the same primary energy because they occurred at the same integral rate per unit solid angle and area. In principle one finds the total energy deposited in ionization from the area  $\int N(x)dx$  under such a shower development curve, multiplied by the rate of energy loss per particle per gram per square centimetre. (The particle numbers were in any case deduced from observations of energy deposition in scintillators.) Fluctuations in shower development mean that the sizes  $N$  plotted on the graph (corresponding to a specified flux) are really r.m.s. values rather than mean values of  $N$  (if  $I \propto E^{-2}$ ), but this should increase the area by only about 7% above the true value, according to typical calculations for proton showers. Model calculations also indicate that, at least near  $10^{17}$  eV, the fact that a shower is inclined to the vertical alters its size only through the greater thickness of overlying air: other factors have an effect much less than 5%. However, one has to complete the graph of  $N$  in the upper atmosphere in order to integrate the area: the curves shown on figure 5 are from the 'Leeds model E10', used in effect as templates to join the points and extrapolate. (Any model so far tested which fits the points beyond shower maximum gives virtually the same area before maximum.) Allowing for the undetected energy does not leave much room for uncertainty, unless a very large proportion of the energy is never radiated as mesons. The actual energies derived for the five curves shown are  $5.5 \times 10^{17}$ ,  $1.7 \times 10^{17}$ ,  $5.5 \times 10^{16}$ ,  $1.6 \times 10^{16}$  and  $5.9 \times 10^{15}$  eV, corresponding to fluxes of  $10^{-11}$ ,  $10^{-10}$ ,  $10^{-9}$ ,  $10^{-8}$  and  $10^{-7}$   $\text{m}^{-2} \text{s}^{-1} \text{sr}^{-1}$ . (One might divide the energies by 1.07 to allow for the effect of fluctuations.) No curves are drawn through the two lowest

series of points. They are clearly steeper than the others, and the results shown from the Tien Shan Mountain and sea level experiments confirm that the attenuation is more rapid for these smaller shower sizes. Aircraft observations of Antonov, Ivanenko, Samosudov & Tulinova (1971) also indicate that these small showers develop higher in the atmosphere than expected, though the statistics are poor.

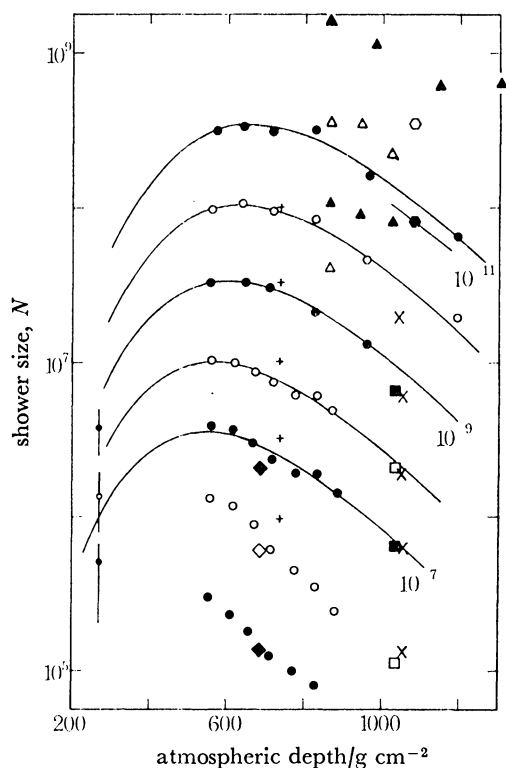


FIGURE 5. The development of showers in the atmosphere. These curves are used to estimate the ionization energy deposited in the atmosphere by those showers which arrive at a particular rate. Each set of points refers to the size ( $N$ ) of shower which arrives at a rate  $I$ , as a function of mass of overlying air. Data from LaPointe *et al.* (1968) for  $I = 10^{-5}, 10^{-6}, 10^{-7}, 10^{-8}, 10^{-9}, 10^{-10}, 10^{-11} \text{ m}^{-2} \text{ s}^{-1} \text{ sr}^{-1}$  are shown by circles (open and filled for alternate sets). Squares refer to results from Kiel, triangles to Volcano Ranch (Linsley 1973), diamonds to Tien Shan, hexagons to Yakutsk, + to Norikura (Miyake *et al.* 1971),  $\times$  to Moscow, and small circles to aircraft observations by Antonov *et al.* (1971). The smooth curves represent the Leeds shower model E10. Note that the two lowest series of points show a behaviour distinctly different from the others.

Our present poor understanding of these smaller showers means that there is no theoretically established conversion to primary energy from shower size in the lower atmosphere near  $10^{15}$  eV, and many groups studying showers in this range have concluded that nuclear interactions must proceed very differently from what is expected by extrapolation from lower energies; with more rapid energy losses by the principal nucleon and very high meson multiplicities. However, noting that the difficulty seems confined to a small range of shower size, and that the more energetic showers fit a more traditional model of interactions, it seems more natural to suppose that many of the showers at energies near  $10^{15}$  eV are produced by very heavy nuclei, but they are not dominant at energies appreciably above  $10^{16}$  eV. This would accord with earlier remarks about the spectrum of iron nuclei. One may thus still regard with caution nuclear interaction models designed to explain shower observations in this range only.



(Alternatively, the energy degradation in nuclear collisions suddenly becomes very high near  $10^{14}$  eV, but reverts to normal above  $10^{16}$  eV.) For the present one notes that shower energies deduced from the Chacaltaya curves have a somewhat wider range of uncertainty near  $10^{15}$  eV, as indicated in figure 4 by two lines in this region.

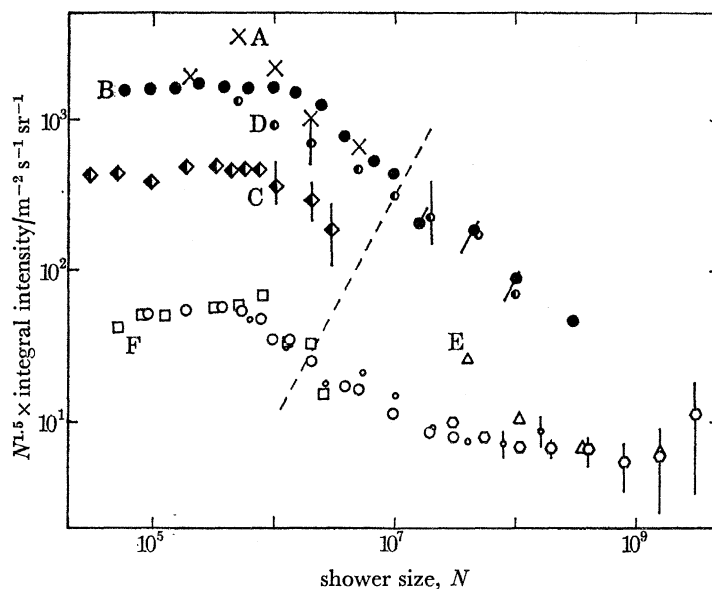


FIGURE 6. Integral size spectrum of showers observed at various altitudes. Note the general agreement in showing a discontinuity in slope. In order of decreasing altitude: A refers to 10000 m (Antonov *et al.*); B, 5200 m (LaPointe *et al.*); C, 3340 m (Hlavac *et al.* 1970); D, 2770 m (Miyake *et al.* 1971); E 1800 m (Linsley *et al.*); F about 100 m including results from Kiel (squares), Moscow S.U. (circles), M.I.T. (small circles) and Yakutsk (hexagons). The oblique dashed line corresponds to an integral flux of  $10^{-8} \text{ m}^{-2} \text{ s}^{-1} \text{ sr}^{-1}$ ; lines parallel to this join points corresponding to the same primary particles observed at different altitudes.

(c) *Evidence of spectral changes between  $10^{15}$  and  $10^{18}$  eV*

Figure 6 shows the spectrum of shower size,  $N$ , obtained by experiments at various altitudes, and demonstrates their agreement in finding a sudden change in the shape of the spectrum at an energy near 3 or  $4 \times 10^{15}$  eV. Although the knee in the  $N$ -spectrum appeared clearly in their experiment, and had previously been seen at sea level (Kulikov & Khristiansen 1958), the Chacaltaya group were uncertain about its interpretation and did not include it in their published energy spectrum. Figure 7 shows approximately how the shower size spectrum should appear at various altitudes near those of the experiments, according to one typical model of shower development ('E10') if the primary particles were always of the same mass (10) and the spectrum steepened from  $\gamma = 2.5$  to  $\gamma = 3.3$  at  $4 \times 10^{15}$  eV. Without insisting on the numerical accuracy of this one model, it serves to show the relation between an energy spectrum and shower size spectra. Aircraft observations (A) are, however, poorly described as though there are much greater fluctuations in shower development than allowed for here.

Although there are evidently calibration differences between the experiments (the fluxes not always varying in order of altitudes), such a change in the energy spectrum is evidently very close to what is observed.

At energies below  $4 \times 10^{15}$  eV,  $\gamma = 2.5$  represents a flatter spectrum than observed for protons in calorimeters at somewhat lower energy, but this is quite reasonable if one is to join

on to the muon-derived spectrum M in figure 4, though the accurate intensity is in doubt because the steep altitude dependence may have led to an underestimate of energy here.

But at energies above the knee, the energy spectrum evidently does not follow a smooth power-law, with  $\gamma = 2.3$ : several sea-level experiments agree in showing a concave  $N$ -spectrum, rather than the slightly convex one that would result from a constant  $\gamma$ . There appears to be a relatively sharp fall in flux up to about  $3 \times 10^{16}$  eV, rather as the dashed line on figure 7, which indicates an energy spectrum with  $\gamma = 3.5$  for a decade from the knee. Beyond  $10^{17}$  eV the spectrum looks less steep, with the exponent  $\gamma$  in the range 2.8 to 3.0, though not well defined as the statistics deteriorate. The very large shower arrays will be seen to give a slope  $\gamma = 3.0$  at the extreme end of the spectrum, though there may be minor irregularities all the way.

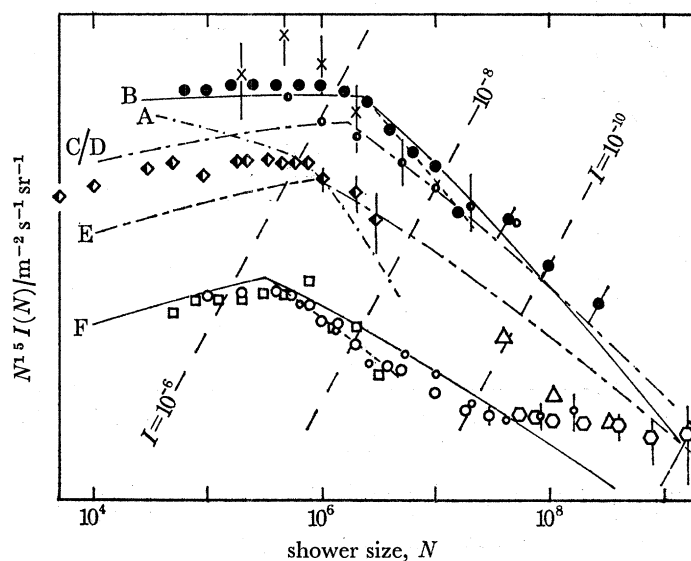


FIGURE 7. Data from figure 6 with curves superimposed to show expected form of shower size spectrum if the primary energy spectrum exponent  $\gamma$  changes from 2.5 below  $4 \times 10^{15}$  eV to 3.3 for higher energies. The full lines B and F refer to depths along the shower axis of 550 and 1080  $\text{g cm}^{-2}$  respectively, appropriate to  $18^\circ$  inclination of the showers at the altitudes of the experiments. C/D refers to 700  $\text{g cm}^{-2}$ , E to 860  $\text{g cm}^{-2}$ , A to 300  $\text{g cm}^{-2}$ . The short steeper dashed lines starting near the bends of lines B and F show the effect of changing  $\gamma$  to 3.5 there.

Qualitatively, the effect is somewhat like the spectral shape first reported from the Volcano Ranch experiment, but the levelling-off, or 'ankle' in the spectrum now seems to occur an order of magnitude lower in energy, and the Volcano Ranch shower size spectrum does not fit in well with those taken at other levels.

(d) *Energy spectrum above  $10^{18}$  eV*

Since it is of particular interest to find whether the flux drops sharply near  $10^{20}$  eV, as expected from the interactions with microwave radiation if the cosmic-ray particles were accelerated more than some tens of million years ago, it will be important to check the energy calibration of the largest shower-detecting arrays. It is difficult to measure the total ionization loss directly, at the level of observation, as the detecting arrays have to cover an area of many square kilometres to collect showers at a tolerable rate, using very widely spaced particle detectors, whereas most of the ionizing particles are within a small distance of the shower axis.

The problem of determining the total number of 'particles' in the shower from samples of particle density taken perhaps 500 m from the shower axis may be judged from figure 8*a* which shows ( $r^2 \times$  particle density) plotted against  $\lg r$ ,  $r$  being the distance from the axis. The area of paper under the curve in a certain distance band directly indicates the number of particles in that range of distance. At the altitude of Volcano Ranch, for which the graph is plotted, half the particles are within about 50 m; and the area under the curve has to be judged from its height at 300 m or more from the axis. Different possible distribution functions which have been used to fit the observations are shown, and it is seen that the result is very sensitive to the choice of distribution function.

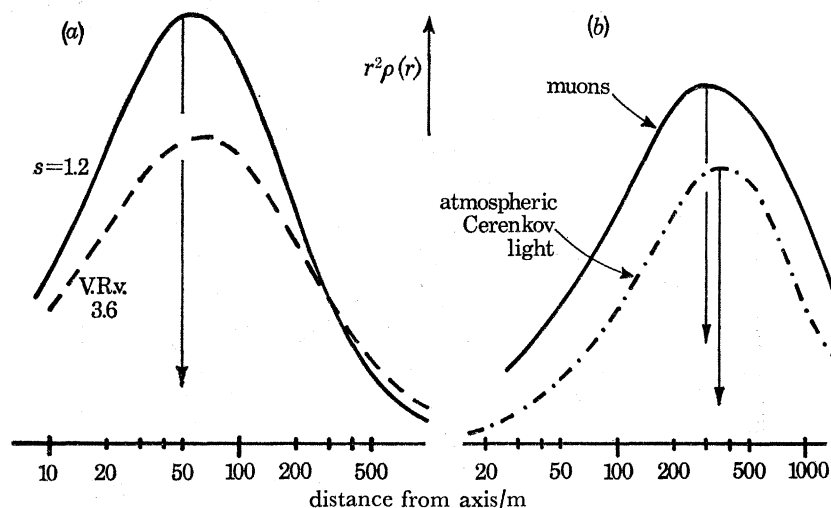


FIGURE 8. Approximate lateral distribution of different shower components, to show extrapolation required in estimating total number of particles  $N = 2\pi \int r^2 \rho(r) d \ln r$  from observations of density  $\rho$  if  $r$  is 300 m or more. Arrows indicate approximate median distances.  $r^2 \rho(r)$  plotted.

(a) Electron component, at altitude of Volcano Ranch, drawn for two shapes of structure function which have been used: a Nishimura-Kamata-Greisen function with  $s = 1.2$ , and a function used by Linsley, referred to by him as V.R.v. 3.6.

(b) Muons and atmospheric Cerenkov photons. Note that these latter have their main contribution near 300 m from the axis.

Figure 8*b* shows the distribution of muons, and of atmospheric Cerenkov photons in a similar way: the Sugar and Yakutsk arrays have made use of these components; and they can be sampled much closer to the median distance of the 'particles', which makes the total shower size estimation much less sensitive to uncertainties in the distributions, though the largest showers are detected at distances near 1000 m.

In this energy range, spectra are available from Volcano Ranch, Yakutsk, Haverah Park and Sugar. Different methods are used to relate the detected signal to primary energy. The calorimetric method of energy determination has been described in connexion with the Chacaltaya experiment: at the lower end of this energy range this overlaps, and the uppermost curve drawn on figure 4 gives an energy  $5.5 \times 10^{17}$  eV for the energy threshold of showers occurring at an integral rate  $10^{-11} \text{ m}^{-2} \text{ s}^{-1} \text{ sr}^{-1}$ . (If fluctuations are taken into account, the energy would only be reduced to about  $5.2 \times 10^{17}$  eV.) The Yakutsk experiment has made the most important contribution of basing its energy determination on the atmospheric Cerenkov light received (in a certain proportion of the showers), which gives a good measure of the total ionization loss by electrons in the atmosphere at higher levels, with only a slight dependence on

details of shower propagation (Dyakonov *et al.* 1973). This method has been available over the energy range  $10^{17}$ – $10^{18}$  eV. The spectrum points plotted by Kerschenholz *et al.* (1973) indicate an integral flux of  $10^{-11} \text{ m}^{-2} \text{ s}^{-1} \text{ sr}^{-1}$  at a shower size  $7.9 \times 10^7$ , and this size their Cerenkov light gives a primary energy of  $5.5 \times 10^{17}$  eV. Thus though  $N$  differs from the Chacaltaya value (apparently being converted to a ‘geiger counter equivalent’), the energy assignment agrees. Haverah Park classifies showers by the signal in a water tank placed 600 m from the axis, and it is necessary to use theoretical models of showers to relate this to primary energy. Models which give a good account of the extensive measurements made on the muon component and the lateral distribution of particles in the shower, up to the present agree closely on the energy assignment. The detailed spectrum of  $\rho_{600}$  published by Edge *et al.* (1973) integrated to give a flux of  $10^{-11} \text{ m}^{-2} \text{ s}^{-1} \text{ sr}^{-1}$  at  $\rho_{600} = 0.80$ , and the models would assign  $6.5 \times 10^{17}$  eV. The Sugar flux (Bell *et al.* 1973*b*) appears to be  $10^{-11} \text{ m}^{-2} \text{ s}^{-1} \text{ sr}^{-1}$  for a shower containing  $4.2 \times 10^6$  muons above their threshold. The same Leeds models assigns an energy  $6.0 \times 10^{17}$  eV to such a number of muons, although the spectrum quoted by the Sydney group, based on the model of Goorevich & Peak (1973), would give an energy  $3.0 \times 10^{17}$  eV.

The only discrepancy is the lower energy assigned by the Sydney model, a model which assumes that little energy goes into pion production in ultra-high energy pion collisions, and which has not yet been tested against so many features of large showers. This difference in the model is the only reason for the lower flux quoted by the Sydney group (see figure 4).

The shape of the energy spectrum may be displayed in terms of the various signals,  $S$ , actually used to measure shower size in order not to prejudge the model. However, a model will be used to suggest the most useful mode of plotting the results. Supposing the primary energy,  $E$ , is related to the signal,  $S$ , by the relation  $E \propto S^\alpha$ , and supposing that the differential spectrum is  $J \propto E^{-3.0}$ , then a plot of  $jS^{2\alpha+1}$  against  $S$  will be a horizontal line, and any deviations in the spectrum will be readily detected. (Here,  $j$  is the differential flux with respect to the variable  $S$ .) Models suggest a suitable value of  $\alpha$ , and there is very little doubt.

For Haverah Park ( $S = \rho_{600}$ ):  $jS^{3.1}$  is plotted (model gives  $\alpha = 1.04$ )

For Sydney ( $S = N_\mu$ ):  $jS^{3.15}$  is plotted (model gives  $\alpha = 1.07$ )

For Yakutsk ( $S = N_e$ ):  $jS^{2.8}$  is plotted (model gives  $\alpha = 0.90$ )

For Volcano Ranch ( $S = N_e$ ):  $jS^{2.9}$  is plotted (model gives  $\alpha = 0.96$ )

For this purpose, the Sydney  $E$  spectrum (Bell *et al.* 1973*b*) was converted back to  $N_\mu$  using the  $N_\mu - E$  graph of Goorevich & Peak (1973). It appears that the average spectral exponent is close to 3.0.

The shower size scales have been alined at the vertical dotted line, which corresponds to the integral flux  $10^{-12} \text{ m}^{-2} \text{ s}^{-1} \text{ sr}^{-1}$ , and the horizontal scales should make the energy scales come nearly into line if the values of  $\alpha$  given above are correct. The actual energy assigned by the different methods varies a little, as shown roughly at the bottom. Some exceptionally large showers have apparently been seen at Volcano Ranch, although the exposure was shorter; it is not yet certain that the structure function is known well enough to deduce the total number of particles, which is quoted. Yakutsk seems to find a rather similar structure function, but at a greater atmospheric depth.

In figure 10, the differential energy spectrum, multiplied by  $E^3$ , is plotted using Haverah Park and Sugar data, but using the Leeds model to convert to  $E$ , as that gave reasonable agreement with other calibrations, and reproduces muon densities in showers observed at Haverah Park. Also plotted are calculated spectra of protons if they are produced with spectrum

$E^{-2.75} dE$ , and have (a) interacted with cosmic microwave (2.7 K) in an expanding universe (using loss-rates calculated by Hillas (1968)), while suffering red-shifts, and (b) have suffered other attenuation processes of the form  $e^{-t/\tau}$ , the sources being constant with time in co-moving volume.  $\tau = \infty$  represents no losses: the protons fill the universe. Negative values of  $\tau$  are equivalent to having stronger sources in the past, as radio-galaxies seem to have been more powerful.

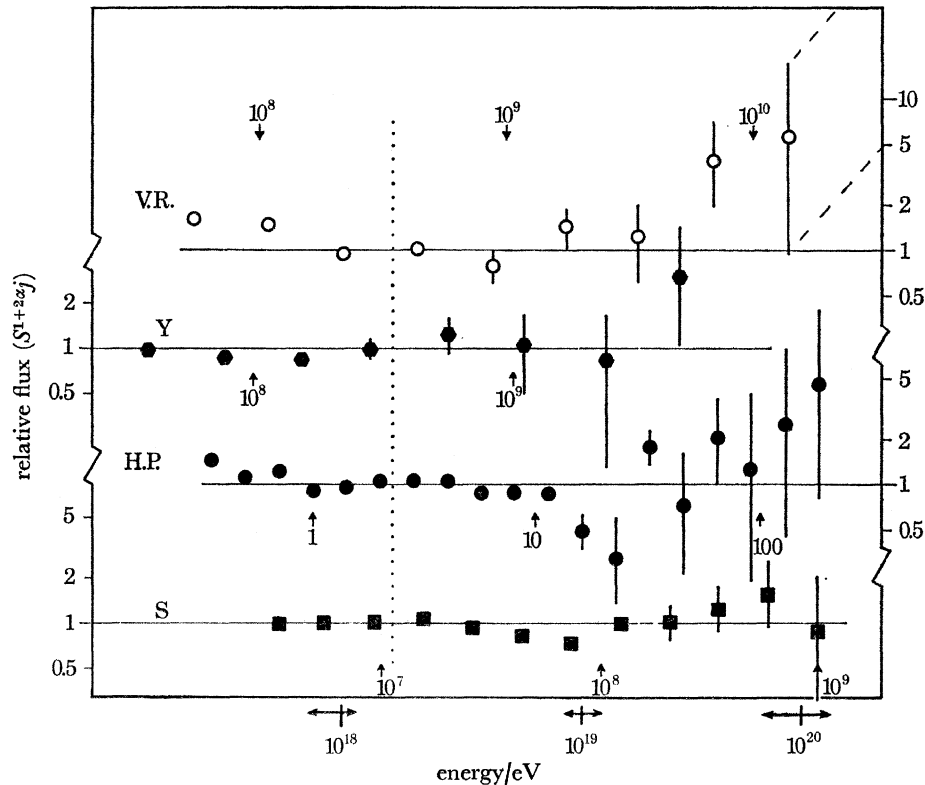


FIGURE 9. Differential shower size spectra at energies above  $3 \times 10^{17}$  eV: comparison of shape of spectra observed at Volcano Ranch, Yakutsk, Haverah Park and Sydney. In each case the spectrum  $j(S)$  of shower 'size'  $S$  is multiplied by an appropriate power of  $S$  (see text) to make the graph horizontal if the primary energy spectrum has exponent  $\gamma = 3.0$ . The numbers refer to different measures,  $S$ , in the four cases: respectively  $N$ ,  $N$ ,  $\rho_{600}$  and  $N_{\mu}$ . Energies are given approximately, for guidance at the bottom, but the different curves may not be precisely aligned.

The results could be reconciled with a universal flux of protons only if the size of the largest showers recorded at Sydney could be reduced by a factor 2, and the largest Haverah Park shower was also modified.

First considering the accuracy of measurement, the spectra quoted for the most energetic showers have indeed steepened in recent years. Edge *et al.* (1973) have noted that, depending on the geometry of the detecting array, the accuracy of size determination can deteriorate with size, leading to a spurious flattening at the end – and this probably caused such a flattening in an earlier published Haverah Park spectrum – but they have estimated the effect to be very small with their present method of shower analysis, and they should see a spectrum cut-off close to its correct position if it exists. In the case of the Sydney and Haverah Park showers, it is just possible that distortions might arise if upward fluctuations in density of muons at very large distances from the axis are more important than we know.



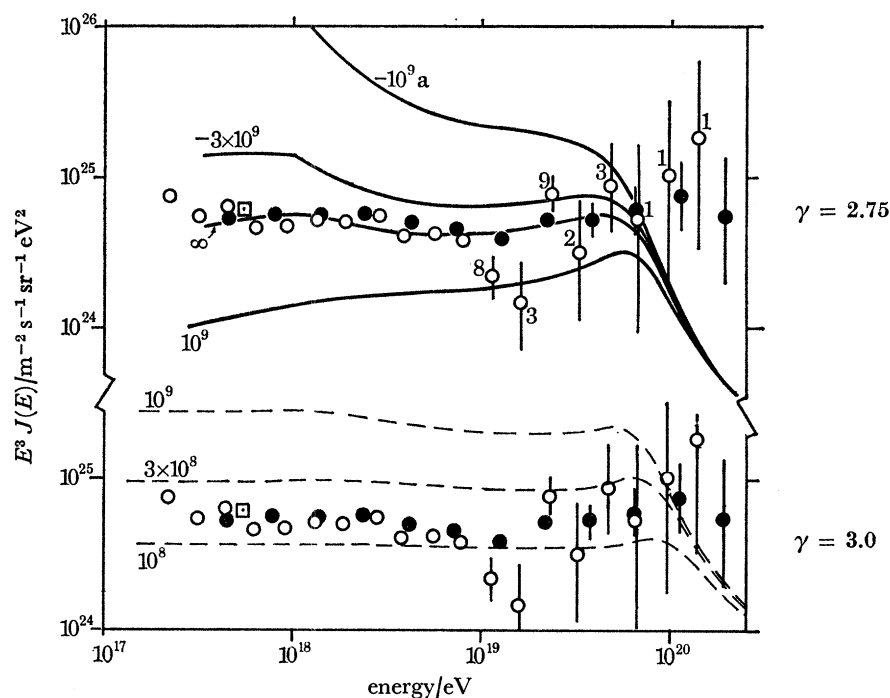


FIGURE 10. Energy spectrum derived from observations of Haverah Park (open circles) and Sydney (black circles) using the Leeds shower model, and one point (square) from ionization loss in atmosphere (see text). Curves are predicted spectral shapes for protons produced with spectral exponent  $\gamma$  and subjected to interaction with cosmic microwaves, assuming leakage or absorption lifetimes  $\tau$ , values of which are attached to the curves. Full lines (above):  $\gamma = 2.75$  and old cosmic rays. Dashed lines (below):  $\gamma = 3.0$  and shorter leakage lifetimes. (Numbers of events are shown on Haverah Park data.)

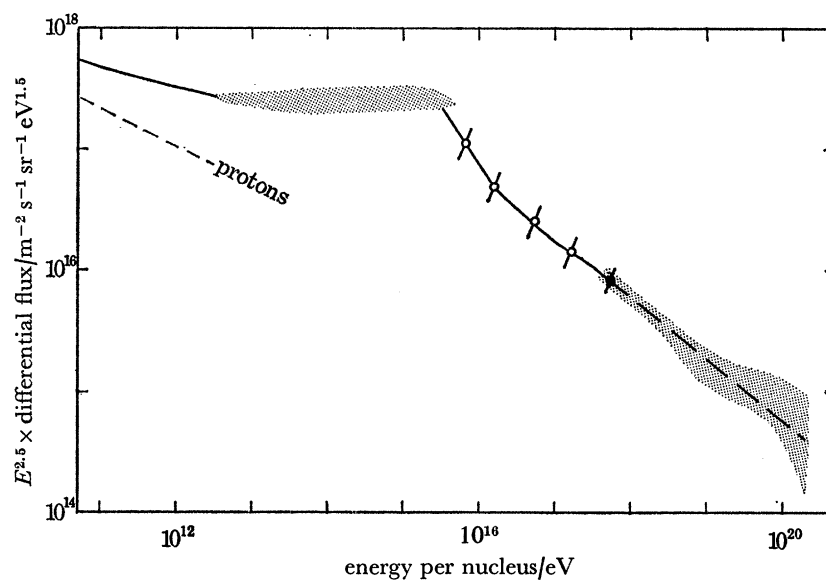


FIGURE 11. Best estimate of the primary differential energy spectrum. The points are converted from the integral intensities  $10^{-7}$  to  $10^{-11}$   $\text{m}^{-2} \text{s}^{-1} \text{sr}^{-1}$  quoted in the text, the solid one being the comparison point of the four large shower experiments. The line is drawn taking into account also the shower size spectrum at sea level.

Alternatively, the model-based conversion from detected signal to primary energy would require alteration, though the conversion used here has been checked against other methods just below  $10^{18}$  eV, as shown earlier. Further calibrations with atmospheric Cerenkov light are to be made at Yakutsk and by Turver's group at Haverah Park. On balance, there seems to be no cut-off, but the evidence can be made more definite after a few more years.

Figure 10 also shows that a production spectrum  $E^{-3.0}$ , combined with a confinement time not much longer than  $10^8$  years, would give a relatively smaller drop in flux near  $10^{20}$  eV; but it would be difficult to maintain a high flux with a short lifetime, and if the Coma cluster were the source, one would expect an appreciable anisotropy.

Finally, the sources cannot have been much stronger at an early cosmological epoch, or the spectrum would be steeper and more curved.

#### (e) Summary

The probable energy spectrum is summarized in figure 11.

Near  $10^{13}$  eV (total energy of nucleus, not energy per nucleon), the primary spectrum including all nuclear species must flatten, apparently with an increase in the proportion of heavy nuclei. Near  $10^{15}$  eV, showers develop higher in the atmosphere than at other energies: they may be caused by very heavy nuclei. At about  $4 \times 10^{15}$  eV, the spectrum steepens sharply,  $\gamma$  changing from 2.5 to 3.5, approximately, but starts to become less steep within a decade, and  $\gamma = 3.0$  from  $3 \times 10^{17}$  to  $3 \times 10^{19}$  eV, with no  $10^{20}$  eV cut-off yet detectable, though the matter cannot be regarded as absolutely settled. One can anticipate a tenfold increase in exposure with further running of the Sugar and Yakutsk arrays, which should show a drop if it exists. If the most energetic particles are protons, their flux lies above the extrapolation of the  $E^{-2.75}dE$  proton spectrum observed below  $2 \times 10^{12}$  eV. The steep slope of the final part of the spectrum means that if these energetic particles belong to the extra-galactic component, that component, extrapolated to lower energies, does not lie below the total flux of cosmic rays. However, the general shape of the spectrum would accord well with the suggestion of Karakula *et al.* (1973) that there is a distinct component present near  $10^{15}$  eV which might be attributed to pulsars.

Energy measurements based on calorimetry and on models which had been fitted in detail agree quite well near  $10^{18}$  eV, even though the fundamental bases of the models are dubious.

### 4. NATURE OF THE PRIMARY PARTICLES

#### (a) Composition below $10^{17}$ eV

There have been no recent changes in the information available on the chemical composition of the primary particles between  $10^{14}$  and  $10^{17}$  eV, although further work by the Polish and French collaboration has strengthened the evidence that fluctuations in the ages of showers near  $10^{16}$  eV observed at sea level are as large as would be obtained from the 'normal' mixture of nuclei as seen at energies below  $10^{12}$  eV. This is taken to imply that protons have not disappeared from the radiation. It is not possible to make a more detailed analysis, and in view of the apparently increasing proportion of iron seen as one starts to approach this energy region from below, one may consider the possibility that the 'mixture' causing fluctuations is principally of very heavy nuclei and very light ones, from two different components of the primary radiation. Most other workers have also concluded that protons are not seriously depleted in

the primary radiation near  $10^{16}$  eV. (Against this view the Sydney group found that bumpy-structured core regions in showers were more noticeable near  $10^{16}$  eV suggesting that contributions from many separate constituents of the primary particle were more important in this energy range, but the Kiel group did not detect a real change and there are no further developments.)

It seems that in the region above  $10^{13}$  eV the proton component of cosmic rays must probably not continue to fall off as steeply as  $E^{-2.75} dE$ .

(b) *Composition above  $10^{17}$  eV*

Linsley has withdrawn his evidence that above  $10^{17}$  eV primaries are protons; he believes that the large fluctuations in shower age that he observed could be due to errors in zenith angle determination. And to offset this change, Turver now does not need heavy primaries to explain the density of muons far from the axis of showers.

Currently, good evidence is being sought, at Haverah Park, of the extent of fluctuations in the depth at which  $10^{18}$  eV showers develop in the atmosphere. Watson & Wilson have found that they can measure real variations in the spread of arrival time of particles at a large distance from the shower axis, and this spread reflects the height up the axis at which the emission of muons is centred. It appears possible to confirm the interpretation by measuring correlated changes in the lateral distribution of particles about the axis. Allan also finds fluctuations in the spread of the radio emission in different showers, as expected if the shower development fluctuates in depth. At this stage all that can be said is that fluctuations of the height of maximum of the order of  $100 \text{ g cm}^{-2}$  seem to be typical.

The meaning of these fluctuations requires more analysis. At one time this would have been taken to reflect the fluctuations in the penetration of a primary proton before it lost the main part of its energy to shower particles, but if the proton mean free path really does become short at such high energies due to an increasing cross-section, the quantitative analysis of fluctuations is less easy. However, even allowing for the fact that Turver and his co-workers have shown that plausible assumptions about shower production by nuclei, which fragment in stages, can result in appreciable fluctuations in the development of showers from heavy nuclei, it still appears likely that the shower energy must be carried by very few particles at some stage, if the tentative experimental results on fluctuations are upheld by further work.

To maintain a galactic origin for the highest energy particles one needs to show they are very highly charged, unless some very special large-scale magnetic field configuration can be accepted.

The author is particularly grateful to many colleagues in the Haverah Park group for discussions of current work, which is reported here.

## REFERENCES (Hillas)

- Antonov, R. A., Ivanenko, I. P., Samosudov, B. E. & Tulinova, Z. I. 1971 *Proc. 12th Int. Conf. on Cosmic Rays, Hobart* **6**, 2194.
- Balasubrahmanyam, V. K. & Ormes, J. F. 1973 *Astrophys. J.* **186**, 109.
- Bell, C. J., Bray, A. D., Denehy, B. V., Goorevich, L., Horton, L., Loy, J. G., McCusker, C. B. A., Nielsen, P., Outhred, A., Peak, L. S., Ulrichs, J., Wilson, L. S. & Winn, M. M. 1973 *a Proc. 13th Int. Conf. on Cosmic Rays, Denver* **4**, 2525; 1973 *b J. Phys. A* (in the Press).
- Clark, G. W., Earl, J., Kraushaar, W. L., Linsley, J., Rossi, B., Scherb, F. & Scott, D. W. 1961 *Phys. Rev.* **122**, 637-54.
- Dyakonov, M. N., Kolosov, V. A., Krasilnikov, D. D., Kulakovskaya, V. P., Lischenjuk, F. F., Orlov, V. A., Sleptsov, I. Ye. & Nikolsky, S. I. 1973 *Proc. 13th Int. Conf. on Cosmic Rays, Denver* **4**, 2384.
- Edge, D. M., Evans, A. C., Garmston, H. J., Reid, R. J. O., Watson, A. A., Wilson, J. G. & Wray, A. M. 1973 *J. Phys. A* **6**, 1612.
- Elbert, J. W., Keuffel, J. W., Lowe, G. H., Morrison, J. L. & Mason, G. W. 1973 *Proc. 13th Int. Conf. on Cosmic Rays, Denver* **1**, 219.
- Goorevich, L. & Peak, L. S. 1973 *Proc. 13th Int. Conf. on Cosmic Rays, Denver* **4**, 2617.
- Greisen, K. 1965 *Proc. 9th Int. Conf. on Cosmic Rays, London* **2**, 609.
- Greisen, K. 1966 *Phys. Rev. Lett.* **16**, 748.
- Grigorov, N. L., Gubin, Yu. V., Rapoport, I. D., Savenko, I. A., Akimov, V. V., Nesterov, V. E. & Yakovlev, B. M. 1971 *Proc. 12th Int. Conf. on Cosmic Rays, Hobart* **5**, 1746.
- Hillas, A. M. 1968 *Can. J. Phys.* **46**, S623.
- Hlavac, T., Nesterova, N. M., Nikolsky, S. I. & Romakhin, V. A. 1970 *Acta. Phys. Acad. Sci. Hungaricae Suppl.* **29**, 1, 521.
- Karakula, S. J., Wdowczyk, J. & Osborne, J. L. 1973 *Proc. 13th Int. Conf. on Cosmic Rays, Denver* **1**, 633.
- Kerschenholz, I. M., Krasilnikov, D. D., Kuzmin, A. I., Orlov, V. A., Sleptsov, I. Ye., Yegorov, T. A., Khristiansen, G. B., Vernov, S. N. & Nikolsky, S. I. 1973 *Proc. 13th Int. Conf. on Cosmic Rays, Denver* **4**, 2507.
- Krasilnikov, D. D. 1973 *Proc. 13th Int. Conf. on Cosmic Rays, Denver* **4**, 2393.
- Kulikov, G. V. & Khristiansen, G. B. 1958 *Zh. Eksper. Teor. Fiz.* **35**, 635.
- Lapikens, J., Martin, R., Reid, R. J. O., Robinson, P. D., Tennent, R. M., Watson, A. A. & Wilson, J. G. 1971 *Proc. 12th Int. Conf. on Cosmic Rays, Hobart* **1**, 316.
- LaPointe, M., Kamata, K., Gaebler, J., Escobar, I., Domingo, V., Suga, K., Murakami, K., Toyoda, Y. & Shibata, S. 1968 *Can. J. Phys.* **46**, S68.
- Linsley, J. 1963 *Proc. 8th Int. Conf. on Cosmic Rays, Jaipur* **4**, 77.
- Linsley, J. 1973 *Proc. 13th Int. Conf. on Cosmic Rays, Denver* **4**, 2518.
- Miyake, S., Ito, N., Kawakami, S., Hayashida, H. & Suzuki, N. 1971 *Proc. 12th Int. Conf. on Cosmic Rays, Hobart* **7**, 2748.
- Ramana Murthy, P. V. & Subramanian, A. 1972 TIFR preprint, Bombay, BC-72-4 CR-MU-6 (72).
- Ryan, M. J., Ormes, J. F. & Balasubrahmanyam, V. K. 1972 *Phys. Rev. Lett.* **28**, 1497, 985.
- Zatsepin, G. T. & Kuzmin, V. A. 1966 *Zh. Eks. Teor. Fiz. Lett.* **4**, 114.